The Materials Research Society (MRS)
XXIV INTERNATIONAL MATERIALS RESEARCH CONGRESS 2015
NACE International Congress-Mexican Section

EFFECT OF AGE-HARDENING ON MICROSTRUCTURE AND MECHANICAL PROPERTIES OF 2024 ALUMINUM ALLOY WITH ALUMINA NANOPARTICLES PRODUCED BY MECHANICAL MILLING.

Carlos Alberto López-Medina. Centro de Investigación en Materiales Avanzados (CIMAV), Miguel de Cervantes 120, Complejo Industrial Chihuahua, México; C.P. 31109. Tel: +52 6144391102. Ingeniería Metal-Mecánica, Universidad Tecnológica de Torreón, Carretera Torreón-Matamoros KM.10 Ejido el Águila, C.P. 27410, Torreón México.clopez@utt.edu.mx.

Humberto Borja Cerda. Ingeniería Metal-Mecánica, Universidad Tecnológica de Torreón, Carretera Torreón-Matamoros KM.10 Ejido el Águila, C.P. 27410, Torreón México.hborja@utt.edu.mx.

Oscar Omar Esquivel Ceniceros. Ingeniería Metal-Mecánica, Universidad Tecnológica de Torreón, Carretera Torreón-Matamoros KM.10 Ejido el Águila, C.P. 27410, Torreón México.oesquivel@utt.edu.mx.

Miguel Ángel Neri-Flores. Centro de Investigación en Materiales Avanzados (CIMAV), Miguel de Cervantes 120, Complejo Industrial Chihuahua, México; C.P. 31109. Tel: +52 6144391102. miguel.neri@cimav.edu.mx

Roberto Martínez-Sánchez. Centro de Investigación en Materiales Avanzados (CIMAV), Miguel de Cervantes 120, Complejo Industrial Chihuahua, México; C.P. 31109. Tel: +52 6144391102. roberto.martinez@cimav.edu.mx

Abstract

Mechanical milling and age-hardening were used to obtain 2024 aluminum alloy reinforced with Al_2O_3 nanoparticles and precipitates. The selected alumina content was 0.0, 1.0, 2.0, 3.0, 4.0 and 5.0 wt.%. Consolidated bulk material were obtained by pressing the milled powder in an uniaxial load, after that sintering and hot extruded using indirect extrusion with a ratio of 1:16 were applied to obtain the final material. The aging heat treatment was applied at 180°C during 4 hours. Structural characterization was carried out by transmission electron microscopy (TEM), scanning transmission electron microscopy (STEM), chemical analysis by characteristic X-ray energy dispersion spectroscopy (EDS), X-ray diffraction (XRD) and differential scanning calorimetry (DSC). The best results were obtained with 2.0 wt.% of alumina that is the critical value of ceramic nanoparticle

reinforcement in this material. At this point the yield and tensile strength were 243.1 and 498.9 MPa respectively. Some of the formed precipitates were: Al_2Cu (θ'), Al_2CuMg (S'), $Al_{20}Cu_2Mn_3$ (T). With 3.0 wt.% or bigger contents of alumina reinforcement particles the agglomeration takes place, and reduce the effectiveness with the strength in the MMC (Metal Matrix Composite). Some strengthening mechanism acting at the same time were: hardening by dispersion of a second phase, the subsequent effect over the dislocations line movement, grain refinement, thermal mismatch between alumina and aluminum matrix, Orowan looping, and intermetallics crystallization.

1. Introduction

Nanotechnology has been used to obtain metal matrix composites (MMC), getting properties that are superior to those of constituent phases and also to satisfy the highest requirements. So far most studies are mainly concerned with mechanical properties of the metal matrix composites reinforced with nanometric ceramic particles [1-2].

According with Angers and Krishnadev[3], the mechanical properties of these composites are influenced significantly by the quantity and reinforcements way of distribution, and also by the nature of the interfaces between the reinforcements and the matrix. By this way, the use of mechanical alloying in order to produce aluminum matrix composites, or other metal-matrix composites, would be considered as a very promising and commercially viable technique, since the MMC's are characterized by a homogeneous reinforcement particles distribution.

In this way Perez-Bustamante et al[4], used a new kind of reinforcement material, the carbon nanotubes (CNT), which include single and multiwalled CNTs. One of the most significant applications was as reinforcement, because of its excellent mechanical properties. The application of Al_2O_3 or SiC reinforced aluminum in the automotive and aircraft industries is gradually increasing for structural parts, where the tribological properties of the material are very important as M. Kok reported [5].

Ruiz-Navas et al.[6] worked with a high energy milling process to produce aluminum matrix composite powders, reinforced with a homogeneous dispersion of carbide particles. In particulate-reinforced composites, some agglomerations of the reinforcement particles damage the mechanical properties. Differences in particle size, densities, geometries, flow, or the development of an electrical charge during mixing, all contribute to particle

agglomeration. A nano-size of the reinforcement particle brings about an increase in mechanical strength, but the tendency of particle clustering also increases [7].

The main focus of this research is the results in the age-hardening behavior with the mechanical and microstructural properties on Al-2024 composite, produced by dispersion of alumina nanoparticles with mechanical milling. Aluminum matrix composite consists of nanometric particles of alumina dispersed into aluminum matrix, these particles interact with precipitates of the alloy because of the ageing heat treatment, strengthening the MMC as a result of several mechanisms like: hardening by dispersion of a second phase, the subsequent effect over the dislocations movement, grain refinement, thermal mismatch between alumina and aluminum matrix, Orowan looping, and intermetallics crystallization (dispersoids).

2. Experimental Procedure

2024 Aluminum alloy and 15nm γ-Al_2O_3 particles were used as raw materials. Chemical composition of the 2024 Al alloy is shown in Table 1. The samples were analyzed with an atomic absorption spectrophotometer. The 2024 aluminum alloy powder was produced by machining a solid extruded bar, with a solution heat treatment condition.

The nanometric particles of γ-Al_2O_3 (mkNano, MKN Al_2O_3-015) have an average size of 15 nm. The chosen alumina content was 0.0, 1.0, 2.0, 3.0, 4.0 and 5.0 wt% respectively. The machined metal shavings were mechanically milled with Al_2O_3 nanoparticles in a high energy horizontal attritor mill (ZOZ CM01Simoloyer) for 10 h in an inert atmosphere with argon. The sample weight was 80 g, using 0.5 ml of methanol as a process control agent. The milling ball to powder weight ratio was set at 20:1. The container and milling media were made from hardened steel.

Consolidated bulk products (40 mm in diameter) were obtained by pressing the milled powder at 950 MPa for 5 minutes under uniaxial load. Pressed samples were next sintered under vacuum (1 torr) for 1 h at 523K after that 2h at 773 K with a heating rate of 50 K/min. Sintering material were held 30 minutes at 823K, and hot extruded into a rod of 10 mm of diameter by using indirect extrusion with a ratio of 1:16. The extruded bars were solution heat treated at 768 K during 3 h, and then water quenched followed by artificial ageing at 453 K during 4 h (T6 condition).

Table 1. *Chemical composition of 2024 Al alloy (wt %).*

Elements	Nominal (wt.%)	Experimental (wt.%)
Al	Balance	Balance
Cu	3.80 - 4.90	4.153
Mg	1.20 - 1.80	0.915
Mn	0.30 – 0.90	0.710
Fe	<0.50	0.191
Si	<0.50	0.131
Zn	<0.25	0.130
Cr	<0.10	0.033
Ti	<0.15	0.045

Mechanical tests, including tensile and microhardness analysis were carried out in the longitudinal direction of the extruded bars at room temperature. The tensile tests were carried out with Instron testing equipment at room temperature and constant displacement rate of 2mm/min. Dogs bone tensile test samples with a gage length of 30mm were prepared in accordance to the ASTM B557M standard. Yield strength at ε=0.2% and maximum strength was measured from the σ-ε plot. Microhardness measurements were done using Future-Tech Corp machine, model FM-7 with load of 50g with 15s of dwell time, average values of at least five points randomly selected for regions in each sample were reported. Microstructural characterization was done by transmission electron microscopy (HRTEM/TEM) JEOL JEM 2200FS operated at 200 kV, X ray diffraction was done in a Panalytical X'Pert Pro diffractometer with CuKα radiation (λ=1.5406 Å) operated at 40 kV and 35 mA in the range of 30-110°, and 5s for collecting time and 0.05° of step size. Scanning electron microscopy was done using a JEOL JSM-7401F, operated at 20 kV with signals of SEM and STEM, the chemical analysis was done by energy dispersive spectroscopy (EDS) using an Oxford Inca X-Ray energy dispersive spectrometer coupled to SEM system, and differential scanning calorimetry (DSC) was done in TA instrument M 2920 DSC equipment. DSC runs were from 50 °C to 550 °C, under dynamic argon atmosphere and heating-cooling rate of 10 °C/min with 50mg for each specimen, cut from tensile extruded bars. Thin foils samples for TEM were prepared from extruded bars by electropolishing, using a mixture of 25 vol. % nitric acid in methanol at 223K and 20 VCD.

3. Results and discussion

3.1 Mechanical Behavior

Mechanical properties are shown in Fig. 1, this plot shows the tensile testing results of the reinforced aluminum in age-hardening condition. The aluminum composite exhibits much higher yield and tensile strengths than the original alloy. The strength of the composite increases, as the weight percent of nanoparticles increase, but once the 2.0 wt. % was exceeded, the strength of composite decreases. Some investigations [8-10] have indicated that the strength of the composites increases with mass fraction of nanoparticles, these nanoparticles could be: Al_2O_3, MoSi, SiC, graphite, and CNTs [8-15]. But once the critical percent of nanoparticles in the composites was exceeded, the strength of MMC was diminished.

According with Table 2, the tensile strength increases from 415 MPa to 498.9 MPa corresponding to an increment of 17% at 2 wt.% of Al_2O_3 nanoparticles, that is considerate the critical value of the reinforcement phase. Comparing 2024 aluminum alloy at T6 condition with this percent of reinforcement the increment was 20.2 % for tensile strength. In this way yield strength was diminished because of the nanoparticles are prone to agglomerate and pores retained in the agglomerated zones, would cause decreasing of the density of the consolidate bulk and the mechanical behavior too.

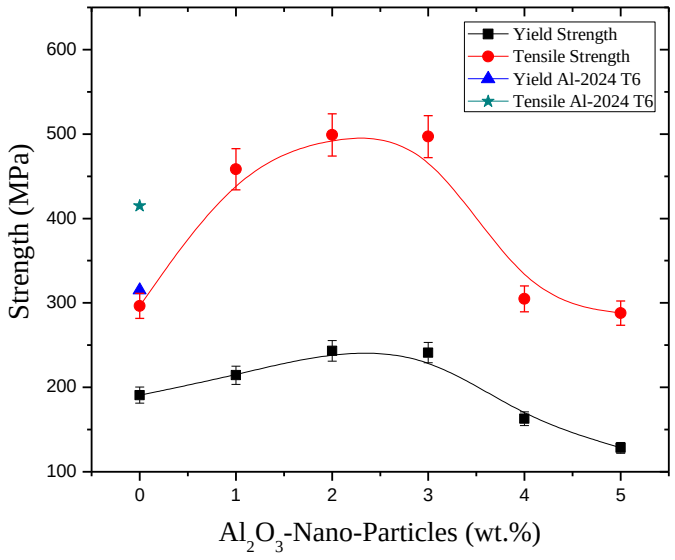

Fig. 1 Tensile Properties of the aluminum composite treated, as a function of wt.% Al_2O_3 nanoparticles, (▲) and (★) Mechanical Properties [16] for Al-2024alloy in ageing condition, T6.

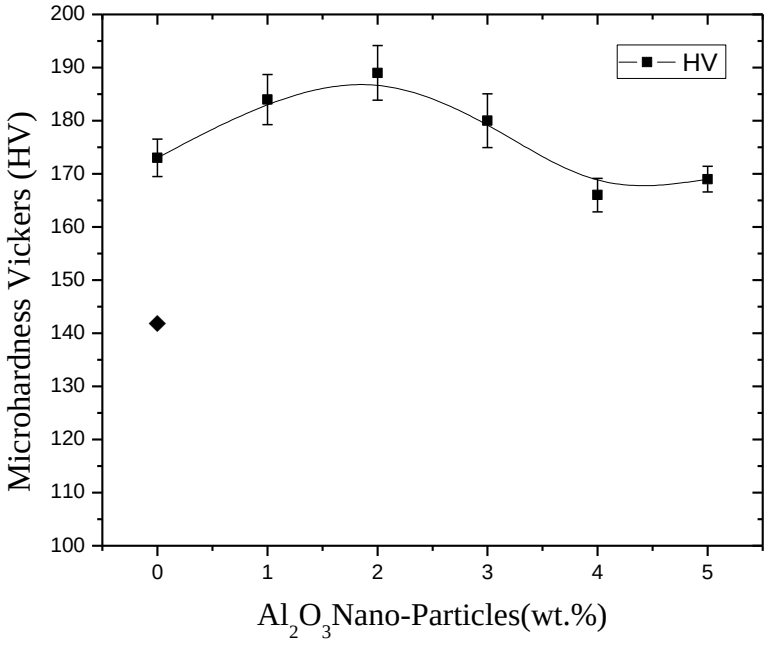

Fig. 2 Micro-hardness Vickers in hardening samples as a function of wt.% Al_2O_3. (◆) Microhardness Vickers (HV) for Al-2024-T6 alloy [16]

The microhardness results for the composites are shown in Fig. 2 with different concentrations of alumina nanoparticles. This plot shows the maximum value (189 HV) in the composite with 2.0 wt. % of alumina. The hardness increases as the alumina content increases, but with contents higher than 3.0 wt.% this property decreases because of the agglomeration of the nanoparticles, and the poor densification in the MMC (Metal Matrix Composite). The maximum hardness was compared with the hardness of pure aluminum alloy, and the average increment was 8.5%, and in contrast with Al-2024-T6 alloy the increase was 33%. It is important to mention that the hardness increase will reduce the powder compressibility, giving porosity in the sintered material. In addition mechanical milling reduces the compressibility of the powders because of the hardening process that occurs during milling. Also Al_2O_3 nanoparticles act as barriers that slow down the diffusion process required for proper sintering as Poirier et al focus on it [10]. A secondary processing such as hot extrusion would help to improve the composite densification but it was not enough to disappear all the imperfections like: voids, cracks or fragile zones in the agglomerated zones.

Table 2 Mechanical properties of 2024-Al alloy at different wt. % of alumina nanoparticles.

** Mechanical Properties of Al-2024-T6 alloy [16].

Material	wt.% Alumina Nanoparticles	Yield Strength (MPa)	Tensile Strength (MPa)	Micro Hardness Vickers (HV)
Al-2024-T6	**	315.0	415.0	142
T0-2024	0.0	190.7	296.5	173
T1-2024	1.0	214.3	458.3	184
T2-2024	2.0	243.1	498.9	189
T3-2024	3.0	241.1	497	180
T4-2024	4.0	162.7	304.8	166
T5-2024	5.0	128.4	288.1	169

3.2 X-ray Diffraction Pattern

The x ray diffraction pattern of 2024 aluminum alloy subjected to increasing wt.% reinforcement alumina is shown in Fig. 3. Several phases are presented in different samples depending the wt.% of the reinforcement in aged condition. Some of the phases that reflect the signal are: the aluminum matrix Al (❖), Al_2CuMg S' (ↄ), Al_2Cu θ' (♦) and $Al_{20}Cu_2Mn_3$ T(□) Those precipitates had been reported in this alloy containing magnesium and manganese as alloying elements[19-20]. It is known that if the phases have nano-size do not appear in x- ray diffraction patterns, so that, no reflections from Al_2O_3 were observed in the MMC pattern. According with XRD pattern Fig. 3, some of the phases like T and S' disappeared as the wt.% of the reinforcement increases, because the thermal activation energy in composites with elevated wt.% reinforcement is higher than in low percent of alumina[17]. In this way the pattern shows that the addition of alumina introduces a lot of interfaces, which reduce the whole concentration of vacancies in the aluminum matrix alloy and therefore the formation of GPB (Guinier-Preston-Begaryatsky) zones are suppressed, these zones give us the S' phase [17-19], who improve the mechanical properties as we shown in Fig. 1 depending on percentage Al_2O_3 reinforcement.

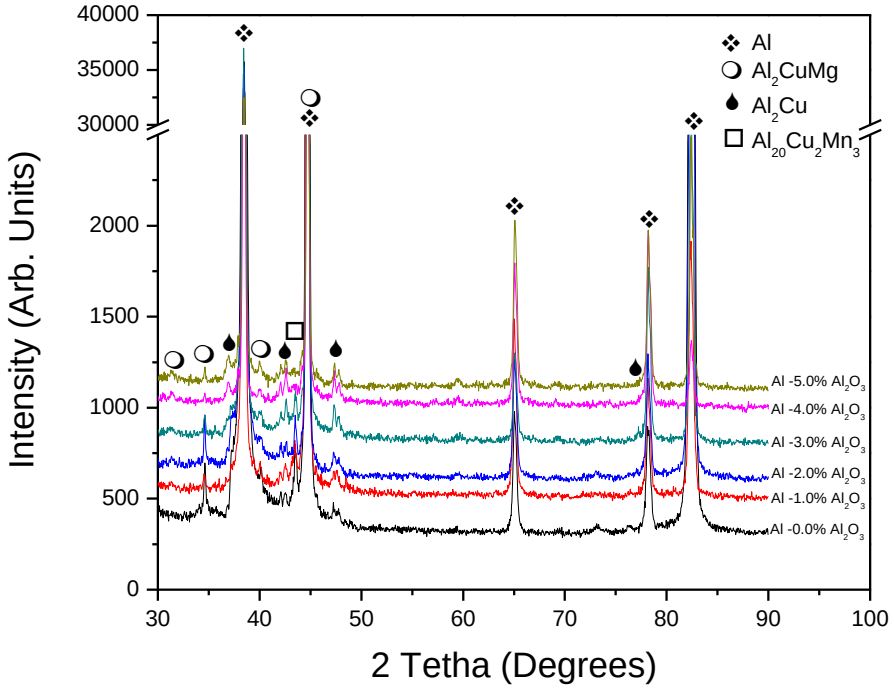

Fig. 3 X ray diffraction Pattern in aged hardening samples as a function of alumina wt.%.

3.3 Thermal Analysis

Fig. 4 shows the DSC curves at different wt.% of alumina nanoparticles in the alloy at the age-hardening condition. In all concentrations of alumina the DSC diagrams differ significantly according with the reinforcement percentage. These curves show several peaks in the range of 50-550 °C. Below 2.0 wt.% of alumina reinforcement, an endothermic peaks appears about 220 °C because of the dissolution of the clusters of GP and GPB zones. The next phenomenon was an exothermic peak due to precipitation of Al_2CuMg intermetallic compound [14-22]. About this kind of alloy, the authors have reported the next sequences [19, 22-28]:

SSS (Saturated solid solution) → GPB (Guinier-Preston-Begaryatsky) → S''→S'/S (Al_2CuMg) [19-22]

SSS (Saturated solid solution) → GP (Guinier- Preston) → θ'' → θ'/θ (Al_2Cu) [24-28]

According these sequences; the first endothermic peak is the dissolution of GP-GPB zones after this, an exothermic peak at 255°C gives a S'/θ' and finally above 400 °C, a second endothermic peak is showed due to dissolution of the S'/θ' precipitates, as predicted by

the aluminum-copper-magnesium diagram [19]. Moreover these phases S''/θ'' and S'/θ' give a peak in hardness because the coherent and semicoherent behavior, increasing internal stress in the crystal lattice [14,22].

At high concentration of reinforcement like 3.0 wt.% of alumina or more, the exothermic peaks do not appears because the nanoparticulates introduces many interfaces, which reduce the whole concentration of vacancies in matrix aluminum, and consequently the formation of GP-GPB zones are suppressed. Successively these zones have been the precursor of the S' and θ' phases, that could affect the mechanical properties as we can view in the Fig. 1 and Fig. 2.

Some theories have been applicable for the exothermic peaks ranging about 450°C. This phenomenon is related with the formation of Al_4C_3, as Y.Zhou et al.[23] demonstrated. In addition, aluminum carbide is formed by the reaction between aluminum and carbon introduced as a process control agent (PCA). This carbide is dispersed throughout the metal with nanometric size, increasing the mechanical strength and refining the microstructure [24-25]. Other authors proposed [25] that the exothermic peak observed during the heating at 420-450 °C was possibly caused by the recovery that should have occurred because of the refining process during mechanical milling.

In this range of temperature for all concentration of reinforcement particles, D.Ying and L.Zhang[30] proposed that endothermic peaks above 450°C were caused by melting of Al-Cu solution with very high Cu content. This solution might be formed during heating process due to inhomogeneous distribution of Al and Cu in the alloy [29].

The thermal analysis illustrates that Al_2O_3 nanoparticles lead to the reduction in the volume fraction of the Guiner-Preston (GP) and Guiner-Preston-Bagaratski (GPB) zones. This decrease is due to the lower vacancy concentration in the matrix of the composite, compared to that in the unreinforced alloy, that were confirmed by XRD and DSC, Figures 3 and 4 [24,31]. Lower vacancy concentration in the composite is due to the large area of nanoparticles-matrix interfaces which act as vacancy sinks. Therefore, the poor vacancy concentration in the MMC, compared to that in the unreinforced alloy is responsible for retarding or for diminishing the formation of GP and GPB zones. Delaying this step, the sequence for producing θ' and S' phases was not enhanced, impoverishing the mechanical behavior. In Fig. 4 the DSC curves corresponding for 4.0 and 5.0 wt.% of Al_2O_3 nanoparticles do not appear in the exothermic peak of the GP and GPB zone formation.

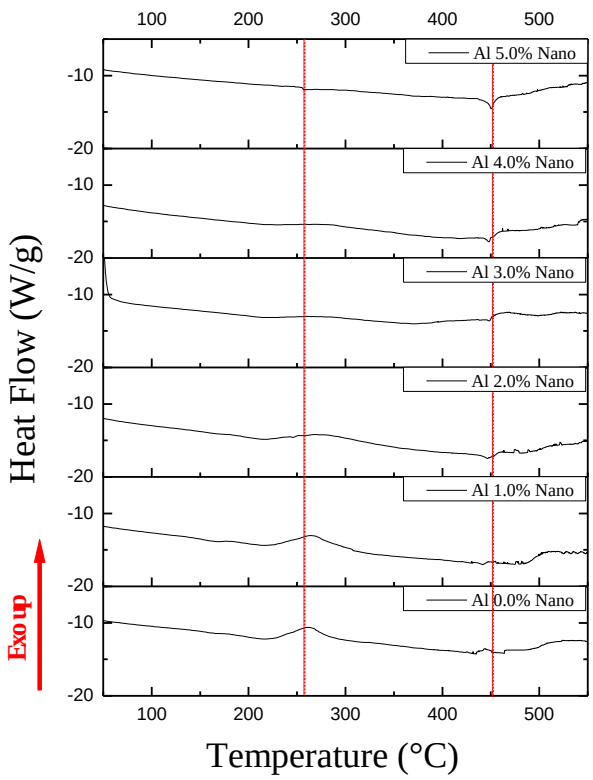

Fig. 4 DSC curves in Al-2024 alloy in the aged hardening as a function of wt.% alumina nanoparticles. DSC conditions were 10 °C/min under flowing argon.

3.4 Microstructural Evolution

The microstructure of the aluminum alloy composite may explain the results obtained on the mechanical properties as the tensile strength and hardness. After mechanical milling, consolidation, hot extrusion and heat treatment processes, the samples were analyzed by STEM, TEM and EDS techniques and some results are shown in Fig. 5 (A and B).The STEM micrographs show the alumina nanoparticles with acicular shape embedded into the aluminum and sometimes agglomerated along the aluminum matrix material. Actually, neither voids nor cracks could be observed, indicating excellent interfacial binding at low concentrations (< 2.0 wt.%) of reinforcement particles.

According with literature [8-10] a decrease of the reinforcement particle size, from micrometric to nanometric scale, carries a superior increase in the mechanical strength, but particles tend to cluster and to agglomerate. It is point out that homogeneous

distribution of the reinforcing particles is essential for achieving the improved properties [10-15].

The results of structural study by STEM, Fig. 5 (C and D) revealed that the crystallite size in the composites is small with nanometric size. The high dislocation activity is the responsible of the acceleration of grain refinement, due to interaction between dislocations and alumina.

In the Fig. 5 the microstructures of the composites, perpendicular to the extrusion axis, explain that the nanoparticles refine the subgrain structure and increase the hardness and strength. The strengths of the composited increased with the mass fraction of particulate. But once the critical value has been exceeded, in this case 2.0 wt.% of Al_2O_3, the strength of composites was decreased. Furthermore the strengthening mechanisms exhibited in the MMC were: the hardening by dispersion of a second phase, the subsequent effect over the dislocations movement, Orowan looping, thermal mismatch between alumina and aluminum matrix, grain refinement, and intermetallics crystallization.

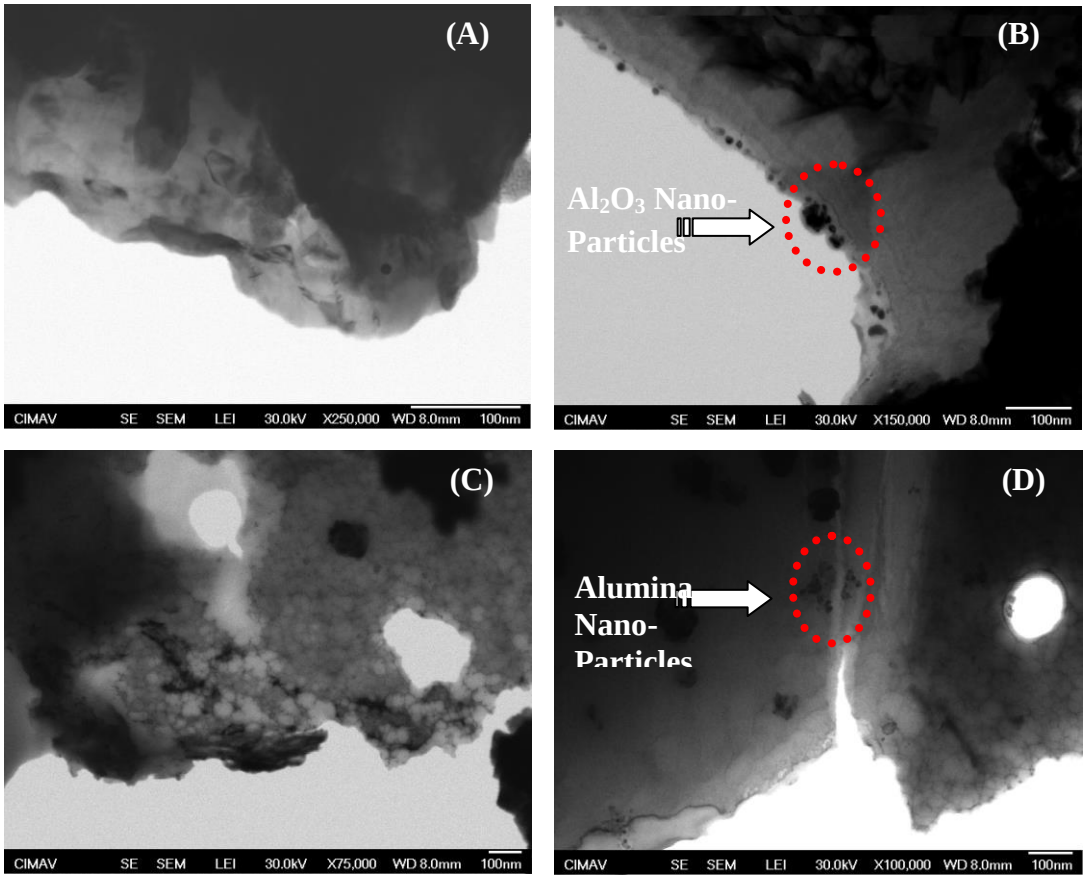

Fig. 5 STEM micrographs of the Al-2024 alloy - 1.0 wt.% Al_2O_3 specimen in aged condition at 180 °C for 2 hr. (A and B) Alumina nanoparticle in the structure embedded into the aluminum matrix, (C and D) Al-2024 alloy - 2.0 wt.% Al_2O_3. Nano-agglomerations of particles take place.

The microstructures of the composite treated by age-hardening were observed using TEM, Fig. 6. A number of needle shaped phases like; Al_2Cu (θ'), Al_2CuMg (S') and $Al_{20}Cu_2Mn_3$ (T) are the main precipitates in the 2024 composite. The chemical composition of those intermetallics were analyzed by EDS, Fig. 6 (B, D, F) confirming the average percentage of elemental composition of these phases reported in this alloy [19-22].

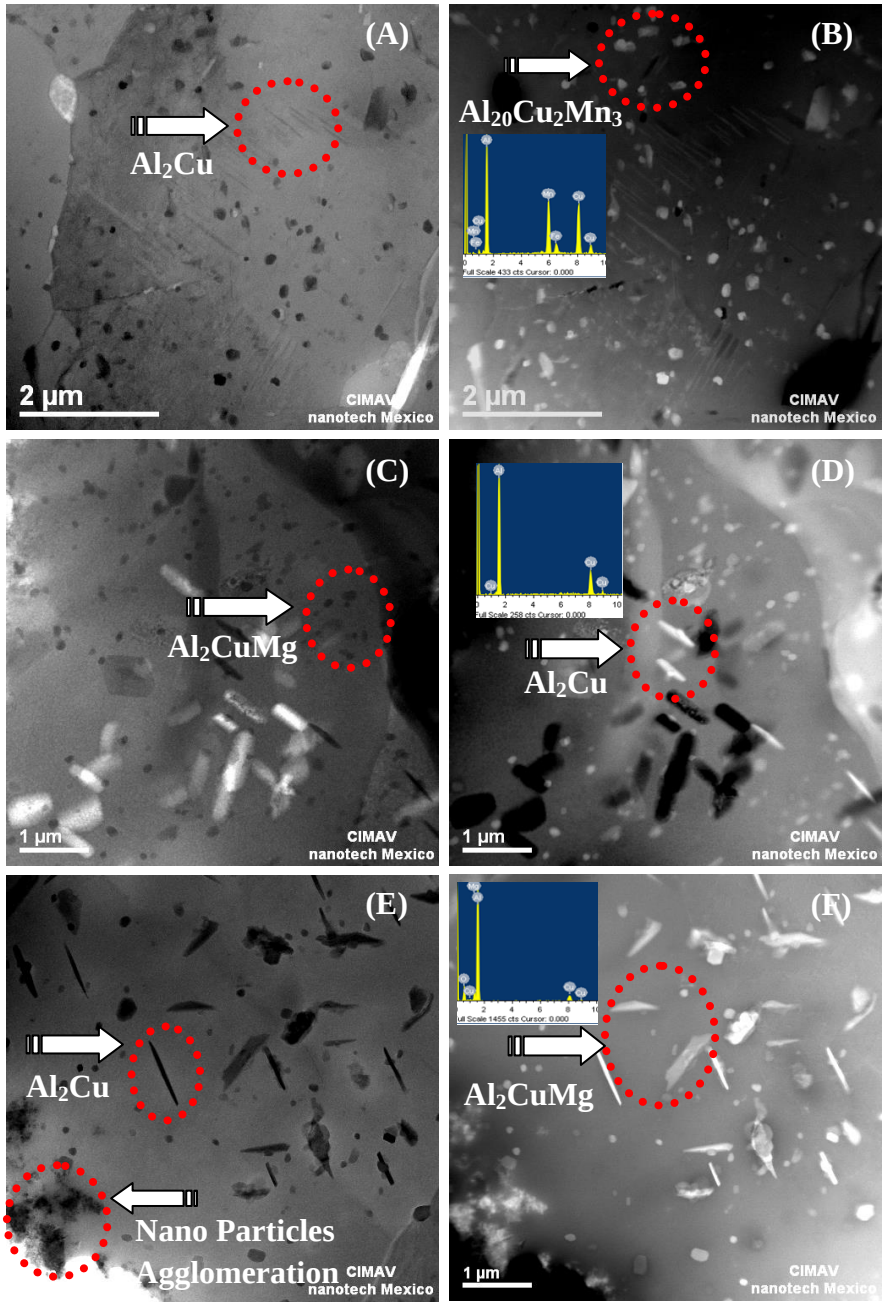

Fig. 6 (A) Bright field, (B) Dark field TEM micrographs of the Al-2024 alloy - 0.0 wt% Al_2O_3 specimen in aged condition. Precipitates like Al_2Cu (θ') and $Al_{20}Cu_2Mn_3$ (T) appear due to the heat treatment. (C) Bright field, (D) Dark field TEM micrographs of the Al-2024 alloy - 1.0 wt.% Al_2O_3 in the same condition the Al_2CuMg (S') come into view. (E) Bright field, (F) Dark field TEM micrographs of the Al-2024

alloy - 3.0 wt.% Al_2O_3. Alumina nano-agglomeration particles in the subgrains structure embedded in the aluminum matrix interacting with S',θ' and T precipitates.

Hence, nano-scale S'/θ' precipitates would be formed after some minutes of ageing, these nanoprecipitates grow and form coherent and semicoherent interface structures with the matrix, rising and increasing its hardness (Table 2) because of the internal stress field near precipitates [14,20-22]. Phases like S and θ lose coherency with the matrix leading to a decrease in mechanical properties.

The presence of $Al_{20}Cu_2Mn_3$ particles can enhance the mechanical properties of Al-Cu-Mn alloy [27-28,33]. This phase appears clearly when the incident direction of the electron beam is parallel to the axis [100] of the aluminum matrix. If this phase is much denser, the mechanical strength is greater [33] as shown in XRD patterns, Fig. 3 and the mechanical results in Table 2.

Generally, in the reinforced composites work different mechanisms at the same time, for example: a high density dislocation are induced in the matrix during temperature changing due to the difference in expansion thermal coefficient, between ceramic phase and aluminum alloy matrix [10-12,18,31-32]. Orowan mechanism leads to dislocation multiplication when nano-scale is used. This means more interaction between the reinforcement and dislocation, and a faster dislocation density increase, as it was viewed in Table 2 with the mechanical properties.

Orowan looping equation calculates the resistance of the second phase to the passage of dislocation from balance between the forcing action on the dislocation and the force coming from line tension acting on both sides of the bulge. It has been modified by Ashby taking into account of the distribution of particles spacing and the size of the particles (Ashby-Orowan eq. 1) [10]:

$$\Delta\tau = 0.84 * \frac{1.2G*b}{2\pi*L} * \ln\frac{r}{b} \qquad \text{eq. (1)}$$

Where $\Delta\tau$ is the increase in shear stress, L is the average inter-particle spacing, G is the shear modulus of the matrix, b is the Burger's vector and r is the average particle radius of Orowan model, defined as the average particle radius measured from polished surface, or intersection radius. This intersection was calculated from particle diameter (~ 15nm for this reinforcement) with equation:

$$r = \frac{D}{\sqrt{6}} \qquad \text{eq. (2)}$$

The average interparticle spacing L is defined in this model as the number of particles seen in a polished surface per unit area. It was calculated from the Volume fraction (Vp) and the intersection radius using this relation [8-10]:

$$L = \left(\frac{\pi * D^2}{6 * V_p}\right)^{\frac{1}{2}} \quad \text{eq. (3)}$$

The increase in shear stress can be converted to an increase in yield strength from:

$$\Delta\sigma_y = M_T * \Delta\tau \quad \text{eq. (4)}$$

Where MT is the Taylor factor, in this case with a value of 3.1[10].

Another strengthening mechanism, working at the same time is the thermal mismatch. According to this when the composite is cooled from sintering, hot extrusion and heat treatment, mismatch strains occur due to difference between the coefficients of thermal expansion of the 2024 aluminum and the alumina nanoparticles (CTE_{2024Al}= 24.7 x 10^{-6} K^{-1} and $CTE_{Alumina}$= 7.5 x 10^{-6} K^{-1})[16]. This thermal mismatch was modeled with Arsenault equation[32], based in the subsequent equations:

$$\varepsilon_{th} = \Delta\alpha * \Delta T \quad \text{eq. (5)}$$

Where ε_{th} is the thermal strain, $\Delta\alpha$ is the difference between the coefficients of matrix thermal expansion and the reinforcement, and ΔT is the temperature change.

The corresponding dislocation density generation (ρ) is found to be [10-12,31-32]:

$$\rho = \frac{B * V_p * \varepsilon_{th}}{b * t * (1 - V_p)} \quad \text{eq. (6)}$$

Where B is a geometric constant that is theoretically between 4 (for reinforcement aspect ratio = ∞) and 12 (for reinforcement aspect ratio = 1), Vp the volume fraction of reinforcement, b the Burger's vector and t the smallest dimension of the reinforcement. The consequent increase in the strength ($\Delta\sigma$) of the MMC can be obtained from [10-12, 31-32]:

$$\Delta\sigma = \alpha * G * \rho^{\frac{1}{2}} * b \quad \text{eq. (7)}$$

For this equation; α is a constant equal to 1.25[10-12] and G is the shear modulus of the matrix.

It is seen that the reinforcement size has a strong impact in the strengthening mechanism. It is known in literature that Orowan effect is insignificant for particles sizes above 1μm

[10,34], but for smaller reinforcement particles in nanoscale, the gains in the strength predicted by thermal mismatch and Orowan looping, increase drastically the mechanical behavior.

At 2 wt.% of reinforcement, alumina nanoparticles have achieved the concentration threshold. It was attributed to three factors: a saturation of the grain boundary with nanoparticles, stopping further grain refinement, a grain boundary embrittlement [10-12], due to nanoalumina aggregates and the reduction in effective nanoparticles content because of the interparticle spacing (L) calculated on the Ashby-Orowan mechanism (eq. 1). It can be understood that the reinforcement has two interacting processes. The first one is a strengthening mechanism, which is dominant at low concentrations of alumina. The second one, which occurs at high levels of alumina nanoparticles, the interparticle spacing (L) pass a critical point where the amount of porosity increases in the MMC [11-15]. In this research the Al_2O_3 critical content was found to be 2.0 wt.% because more over this value, the probability of clustering is thought to be a major factor, which alters the microstructure and impoverishing the mechanical strength.

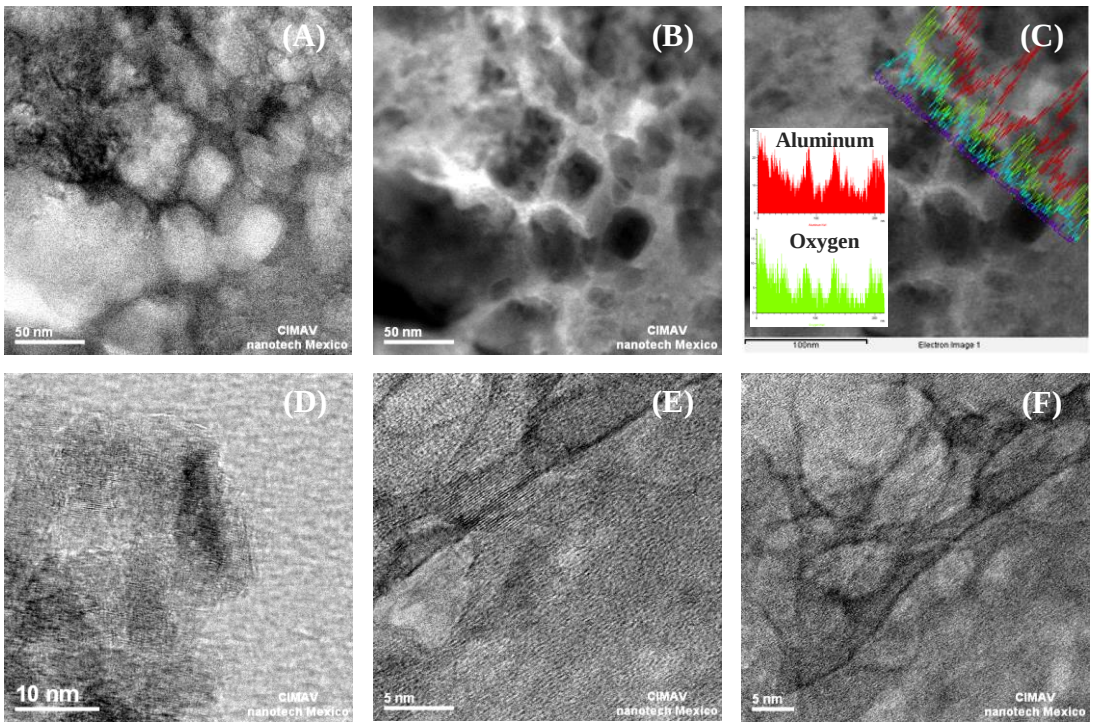

Fig. 7 (A) Bright field, (B) Dark field TEM micrographs of the Al-2024 alloy- 3.0 wt% Al_2O_3 specimen in ageing condition. Alumina nano-agglomerated particles in the aluminum matrix alloy. (C) Electron micrograph in the same zone showing EDS line scanning for Al-O to be evidence the alumina nano-particles. (D, E and F) HRTEM micrographs showing a closer view of alumina nano-particles in the aluminum composite.

A common characteristic in the microstructure of the material with different wt.% of reinforcement is that coarse θ' precipitates are densely distributed in the regions where quite a few nanoparticles exist. The θ' and S' precipitates are sparsely distributed in the regions where nano-agglomerations particles are dense, as viewed in Fig. 6 (E and F).

The interface is regarded to act as an aggregation site of the alloying elements, and causes reduce solute atom concentration in the composite matrix. When the precipitates in materials are tiny and uniformly dispersed, they can pin dislocation more effectively and impede the movement of the dislocations [18], so that the resistance of the material increases, Table 2. This is one of the main reasons why ultimate strength of the nanoparticle reinforced composite is higher than in the original 2024 alloy. In that way the thermal mismatch between Al_2O_3 particle and matrix is very small during temperature change and could hardly induce dislocations near to the nanometric reinforcement.

In the micrographs of TEM shown on Fig. 7 (A and B) were analyzed the distribution and the morphology of Al_2O_3 nanoparticles. To identify the reinforcement phase, the elements of the alumina: oxygen and aluminum were found using EDS line scanning, in the metal matrix composite, Fig. 7 C. In this line, the agglomeration of particulates due to an increasing wt. % of reinforcement appears. In Fig. 7 (D, E and F), HRTEM was applied to show the shape of the nanoalumina and how it is embedded into the matrix without voids or cracks in the interfaces. The morphology of nanoparticles illustrates irregular and acicular shapes in the agglomerated particles. Nevertheless it is important to point out that if a big amount of nanoparticles agglomerated occurs, the MMC could reduce the relative density, consequently their mechanical properties get down and the agglomerations provide sites for crack initiation, from pores in the middle of the agglomerations, and bad adhesion with this zone and the matrix. At this point voids nucleate from some inclusion in the matrix, grow, coalesce and give the fracture of the material[22-24, 34-37]. Khorshid et al. [12] noted that cracks generally initiate from interfaces between of matrix and reinforcement. By increasing the amount of nanoparticles, the nucleation crack sites increase. When various nucleation sites are active, adjacent cracks coalesce and fracture occurs before they have an opportunity to grow and can form larger size dimples.

4. Conclusion

Working with mechanical milling technique and age-hardening treatment, Al_2O_3 nanoparticles can be introduced to the 2024 aluminum matrix precipitating several phases

like: θ', S' and T. The research was focused that the nanometric reinforcement, and the heat treatment will improve the yield and tensile strength until 243.1 and 498.9 MPa respectively, with 2.0 wt.% of Al_2O_3 nanoparticles. This amount was considerated as a critical value for the reinforcement ceramic phase. On the other hand, with 3.0 wt.% or greater values in alumina reinforcement, the agglomeration takes place, and reduces the effectiveness in the strength in the MMC. In this concentration of reinforcement phase, the exothermic peaks in DSC do not appear at ~250 °C, because the Al_2O_3 nanoparticulates introduce many interfaces, which reduce the whole concentration of vacancies in matrix aluminum and consequently the formation of GPB zones was suppressed. These zones, promote the phase precipitation of S' and θ' affecting the mechanical properties. The most important mechanisms were: the hardening by dispersion of a second phase, thermal mismatch between 2024 aluminum alloy and alumina, intermetallic precipitations, and the Orowan strengthening by Al_2O_3 nanoparticles, but when the hardened powder particles limited the plastic deformation, a poor densification appears and gives the quantity of sites for crack initiation, pores and bad adhesion with the matrix that diminished the mechanical properties. Also it was shown by TEM that the crystallite had a nanosize shape into the aluminum matrix, revealing a grain refining process.

Acknowledgements

The authors sincerely acknowledge for their support to CONACYT and Air Force Office of Science Research, Latin America. Contract No. FA9550/06/1/0524. Thanks to W. Antunez-Florez, C. Carreño-Gallardo, I. Estrada-Guel, K.Campos-Venegas, Torres-Moye, D. Lardizabal-Gutiérrez and R. Torres-Sánchez for their technical assistance.

References

[1] H.T. Son, T.S. Kim, C. Suryanarayana, B.S. Chun. Homogeneous dispersion of graphite in a 6061 aluminum alloy by ball milling. Materials Science and Engineering 2003.

[2] M. Sherif El-Eskandarany. Fabrication and characterizations of new nanocomposite WC/Al_2O_3 materials by room temperature ball milling and subsequent consolidation. Alloys and compounds 2005.

[3] R. Angers, M.R. Krishnadev et al. Characterization of SiC/2024 aluminum alloy composites prepared by mechanical processing in a low energy ball mill. Materials Science and Engineering A 1999.

[4] R. Perez-Bustamante, I-Estrada-Guel, W. Antunez-Flores at al. Novel composites aluminum-multiwalled carbon nanotubes. Alloys and Compounds 2006.

[5] M. Kok. Production and mechanical properties of Al_2O_3 particle-reinforced 2024 aluminum alloy composites. Materials Processing Technology 2004.

[6] E.M. Ruiz-Navas, J.B. Fagagnolo et al. One step production of aluminum matrix composite powders by mechanical alloying. Composites Part A, applied science and manufacturing, 2006.

[7] J.B. Fagagnolo, M.H. Robert, J.M. Torralba, Mechanically alloyed AlN particle-reinforced Al 6061 matrix composites. Materials Science and Engineering A, 2006.

[8] Yung-Chang Kang, Sammy Lap-Ip Chan. Tensile properties of nanometric Al_2O_3 particulate-reinforced aluminum matrix composite. Materials chemistry and physics, 2004.

[9] M. Sameezadeh, M. Emamy, H. Farhangi. Effects of particulate reinforcement and heat treatment on the hardness and wear properties of AA 2024-$MoSi_2$ nanocomposites. Mater and Desing, 2010.

[10] Dominique Poirier, Robin A.L. Drew, Michel L.Trudeau, Raynald Gauvin. Fabrication and properties of mechanically milled alumina/aluminum. Materials Science and Engineering A 2010.

[11] M. Rahimian, N. Ehsani, N. Parvin, H. R. Baharvandi. The effect of sintering temperature and the amount of reinforcement on the properties of Al-Al_2O_3 composite. Materials and Design 2009.

[12] M.Tabandeh Khorshid, S.A.Jenabali, M.M. Moshksar. Mechanical properties of tri-modal Al matrix composites reinforced by nano-and submicron sized Al_2O_3 particulates developed by wet attrition milling and hot extrusion. Materials and Design 2010.

[13] R. Deaquino-Lara, I. Estrada-Guel, G. Hinojosa-Ruiz, R. Flores-Campos, J.M. Herrera-Ramírez, R. Martínez-Sánchez. Synthesis of aluminum alloy 7075-graphite composites by milling processes and hot extrusion. Journal of Alloys and Compounds 2011.

[14] H. J. Choi, B.H. Min, J.H. Shin, D.H. Bae. Strengthening in nanostructured 2024 aluminum alloy and its composites containing carbon nanotubes. Composites: Part A 2011.

[15] Hai Su, Wenli Gao, Zhaohui Feng, Zheng Lu. Processing, microstructure and tensile properties of nano-sized Al_2O_3 particle reinforced aluminum matrix composites. Materials and Design 2011.

[16] www.matweb.com, Mechanical Properties of Al-2024 in a solid solution state and T6.

[17] Jiang Longtao, Zhao Min, Wu Gaohui, Zhang Qiang. Aging behavior of sub-micron Al_2O_3p/2024 Al composites. Materials Science and Engineering A, 2005.

[18] Xiufang Wang, Gaohui Wu, Dongli Sun, Changjiu Qin, Yunlong Tian. Micro-yield property of sub-micron Al_2O_3 particle reinforced 2024 aluminum matrix composite. Materials Letters 2004.

[19] S.C. Wang, M. J. Starink. Precipitates and intermetallic phases in precipitation hardening Al-Cu-Mg-(Li) based alloys. International Materials Reviews, 2005.

[20] S.Cheng, Y.H. Zhao, Y.T. Zhu, E. Ma. Optimizing the strength and ductility of fine structured 2024 Al alloy by nano-precipitation. Acta Materialia 2007.

[21] L. del Castillo, E.J. Lavernia. Microstructure and mechanical behavior of spray-deposited Al-Cu-Mg(-Ag-Mn) alloys. Metallurgical and materials transactions A 2000.

[22] T.S. Parel, S.C. Wang, M.J. Starink. Hardening of an Al-Cu-Mg alloy containing Types I and II S phases precipitates. Materials and Design 2010.

[23] Y.Zhou, Z.Q. Li. Structuctural characterization of a mechanical alloyed Al-C mixture. Alloys and compounds, 2006.

[24] M. Jafari, M.H. Abbasi, M.H. Enayati, F. Karimzadeh. Mechanical properties of nanostructured Al2024-MWCNT composite prepared by optimized mechanical milling and hot pressing methods. Advanced Powder Technology 2012.

[25] J.B. Fagagnolo, D.Amador, E.M. Ruiz-Navas, J. Torralba. Solid solution in Al-4.5% Cu produced by mechanical alloying. Materials Science and Engineering A, 2006.

[26] S. Arakawa, T. Hatayama, K. Matsugi and O. Yanagisawa. Effect of heterogeneous precipitation on age-hardening of Al_2O_3 particles dispersion Al-4mass%Cu composite. Scripta Materialia, 2000.

[27] A.K. Mukhopadhyay. Coprecipitation of Ω and σ phases in Al-Cu-Mg-Mn alloys containg Ag and Si. Metallurgical and Materials Transactions A 2002.

[28] A.K. Mukhopadhyay, G. Eggeler, B. Skrotzki. Nucleation of Ω phase in an Al-Cu-Mg-Mn-Ag alloy aged at temperatures below 200 °C. Scripta Materialia 2001.

[29] D.L. Zhang, d. Y. Ying. Solid state reactions in nanometer scaled diffusion couples prepared using high energy ball milling. Materials Science and Engineering A 2001.

[30] D.Y. Ying, D.L. Zhang. Solid-state reactions between Cu and Al during mechanical alloying and heat treatment. Journal of alloys and compounds 2000.

[31] S.M.R. Mousavi Abarghouie, S.M. Seyed Reihani. Aging behavior of 2024 Al alloy-SiCp composite. Materials and Design 2010.

[32] R.K. Everett, R.J. Arsenault. Metal matrix composites: mechanisms and properties. Boston Academic Press; 1991 P.92.

[33] Zhongwei Chen, Pei Chen, Shishun Li. Effect of Ce addition on microstructure of $Al_{20}Cu_2Mn_3$ twin phase in an Al-Cu-Mn casting alloy. Materials Science and Engineering A 2012.

[34] Z. Razavi Hesabi, A. Simchi, S.M. Seyed Reihani. Structural evolution during mechanical milling of nanometric and micrometric Al_2O_3 reinforced Al matrix composites. Materials Science and Engineering A 2006.

[35] I. Estrada-Guel, C. Carreño-Gallardo, R. Martínez-Sánchez. Effect of carbon nanoparticles addition on the mechanical properties of aluminum composite prepared by mechanical milling and leaching process. Journal of Alloys and Compounds 2011.

[36] Z. Razavi Hesabi, H.R. Hafizpour, A. Simchi. An investigation on the compressibility of aluminum/nano-alumina composite powder prepared by blending and mechanical milling. Materials Science and Engineering A, 2006.

[37]I. Estrada-Guel, C. Carreño-Gallardo, D.C. Mendoza-Ruiz, M. Miki-Yoshida, E. Rocha-Rangel, R. Martínez-Sánchez. Graphite nanoparticle dispersion in 7075 aluminum alloy by means of mechanical alloying. Journal of Alloys and Compounds 2011.